3D flow of suspension of Graphene nanoparticles with different temperature of water over a Slendering stretching sheet

P. Durga Prasad[#1], S. Vijayakumar Varma[#1], R. Sivaraj[2], C.S.K. Raju[*3]
[#1,2]Department of Mathematics, Sri Venkateswara University, India.
[*2]Department of Mathematics, School of Advanced Sciences, VIT University, Vellore, India, India.
[*3]Department of Mathematics, GITAM School of Technology, Bangalore, India.

Abstract: *The present study investigates on the three dimensional MHD flow of a nanofluid across a slendering sheet saturated with porous layers of a suspension of graphene nanoparticles. The primitive objective of this proposed analysis is characterizing the non-uniform energy gain or drop. In the present simulation the graphene-water based nanoparticles have been used at two different temperatures namely* $10^0 C$ *and* $50^0 C$. *Runge-Kutta-Feldberg integration method is used to solve the non-dimensional governing equations of this study. The characteristics of velocity, temperature boundary layers in the presence of graphene-water nanoparticles are presented for various values of heat source/sink, volume fraction, porosity, and wall thickness. Moreover, the Nusselt number in terms of heat transfer are also estimated and discussed for aforesaid physical parameters. Results indicate that higher heat transfer rates are observed in case of graphene-water nanoparticle at* $50^0 C$ *compared with* $10^0 C$.

Keywords: *Magnetohydrodynamic, Porous media, Graphene Nanoparticles, Slendering sheet.*

I. INTRODUCTION

Graphene has two-dimensional extended honeycomb network of sp2-hybridized carbon atoms, chemical properties, high electron mobility, high thermal conductivity and excellent mechanical properties. Recently, after the extraction of a single layer of graphene, it is being reported that graphene also can be used for field emission applications. The sharp edges of graphene can emit electrons with the help of an external electric field [1]. The few-layer graphene is found as a good field emitter where the field amplification factors can be raise up to several thousand [2]. Ghosh et al. [3] examined heat conduction in graphene by experimental study and theoretical interpretation. The field emission property of graphene has been improved by treating it under different atmospheres. Recently, theoretical investigation of Mao [4] has reported that wider graphene nano-ribbon can give a large field-emission current density.The suspended portion of graphene served as several essential functions such as (i) accurately determining the amount of power absorbed by graphene through the calibration procedure, (ii) forming two-dimensional in-plane heat front propagating toward the heat sinks and (iii) reducing the thermal coupling to the substrate through the increased micro and nano scale corrugations. TesseyTheres and Ramaprabhu[5] reported that the field emission properties of metal oxide nanoparticle-decorated graphene.Haque et al. [6] experimentally investigated the thermal characteristics of nanofluid with graphene and multi-wall carbon nanotubes.

Cortell [7] discussed the magnetohydrodynamic flow and radiative nonlinear heat transfer of a viscoelastic fluid over a stretching sheet with heat generation/absorption. Raju et al. [8] portrayed the heat and mass transfer in magnetohydrodynamicCasson fluid over an exponentially permeable stretching surface. Hayat et al. [9] investigated the MHD three-dimensional (3D) flow of nanofluid with velocity slip and nonlinear thermal radiation. Aninasaunet al. [10] proposed the unequal diffusivities case of homogeneous-heterogeneous reactions within viscoelastic fluid flow in the presence of induced magnetic-field and nonlinear thermal radiation. They reported the solutions of Newtonian fluid flows with different flow characteristics. Brownian motion and thermophoresis are the heat transfer mechanism of movement of small particles in the way of falling thermal gradients and affects the small particles related with the bulk surfaces. It has wide range applications in different arenas such as like nuclear safety processes, environmental, hydrodynamics, aerospace and atmosphere pollution aerosol technology etc. Nelson [11] was first studied the dynamic theory of Brownian motion. Babu

and Sandeep [12] discusseda three-dimensionalmagnetohydrodynamic slip flow of a nanofluid over a slendering stretching sheet with Brownian motion and thermophoresis effects.

A nanofluid is a fluid in which nanometer-sized particles are suspended in a convectional heat transfer fluid to improve the heat transfer characteristics. Nanofluids are homogenous combination of base fluid and nanoparticles suspended metallic/non-metallic particles. It can change the transport properties and thermal conduction characteristics of the common base fluids include water, organic liquids (e.g. tri-ethylene-glycols, ethylene, and refrigerants), lubricants and engine oils, polymeric solution and other common liquids. In fact these enable to enhance thermal conductivity based on the properties of the nanoparticles. The nanoparticle is distributive part of any material whose diameter is aboutapproximately 5 to 15 mm. The rate of heat transfer due to the nanoparticles is dependent on various factors such as number of dispersed particles, shape of the particles and material type of nanoparticles. Nanofluids have potentially useful in many applications in heat transfer including pharmaceutical processes, fuel cells, microelectronics, chiller, hybrid-powered engines, domestic refrigerator, heat exchanger, grinding, machining and in boiler flue gas temperature reduction. It is found that the enhancement rate of the heat and mass transfer are high in case of nanoparticle instead of base fluid. Pioneering work in the field of nanofluid has been performed by Choi [13] explained that the nanoparticles increases the thermal conductivity of base fluids and therefore substantially enhances the heat transfer characteristics of the nanofluid. Sheikholeslami and Ganji [14] numerically examined the nanofluid flow and heat transfer between parallel plates considering Brownian motion using differential transformation method (DTM). Malvandi et al. [15] analysed the thermophoresis and Brownian motion effects on heat transfer enhancement at film boiling of nanofluids over a vertical cylinder. Fani et al. [16] investigating the effect of Brownian motion and viscous dissipation on the nanofluid heat transfer in a trapezoidal micro channel heat sink. Angayarkanni et al. [17] reviewed the recent experimental and theoretical developments in nanofluids and summarised the role of Brownian motion, interfacial resistance, morphology of suspended nanoparticles and aggregating. Later, Khan and Aziz [18] studied the boundary layer nanofluid flow over a vertical surface with constant heat flux. Makinde et al. [19] explained the mixed convective magnetohydrodynamic flow in a vertical channelfilled with nanofluids. Makinde et al. [20] portrayed Entropy analysis of thermally radiating magnetohydrodynamic slip flow of Cassonfluid in a micro-channel filled with saturated porous media.Kim et al. [21] introduced a new friction factor to depict the effect of nanoparticles on the convective instability and the heat transfer characteristics of the base fluid.Recently, the authors [24-27] are investigated flow over various geometries (cone or plate or sheet) filled with various type of nanoparticles.

In view of these facts the present study focuses on the numerical investigation of three dimensional flows over the porous layers slendering sheet with non-uniform heat source or sink considering graphene-water nanoparticles have been incorporated with the proposed mathematical model. The boundary layer equations given as a set of partial differential equations (PDEs) are first changed into non-linear ordinary differential equations (ODEs) ahead being solved numerically via Runge-Kutta-Feldberg integration method. The effects of the governing flow parameters on the velocity, temperature profiles have been discussed and presented in tables and graphs.

II. MATHEMATICAL FORMULATION

In the present analysis, we consider three dimensional, electrically conducting hydromagnetic slip flow of nanofluid over a slendering stretching sheet (see; Fig. 1) by assuming $z = J\left(x + y + c\right)^{(1-n)0.5}; n \neq 1.$ In addition, it is considered that the sheet is followed with a porous medium and magnetic Reynolds number is very low. The slip conditions also applied on velocity, temperature field along with non-uniform heat source parameter. In the present numerical simulation, we consider the water as a base fluid and graphene as nanoparticles at temperatures 10^0 and 50^0, respectively. The thermo physical properties of base fluid and nanoparticles at different temperatures are depicted in Table 1. The mathematical analysis and considered that the grapheme nanoparticles and base fluid are in thermal equilibrium condition.

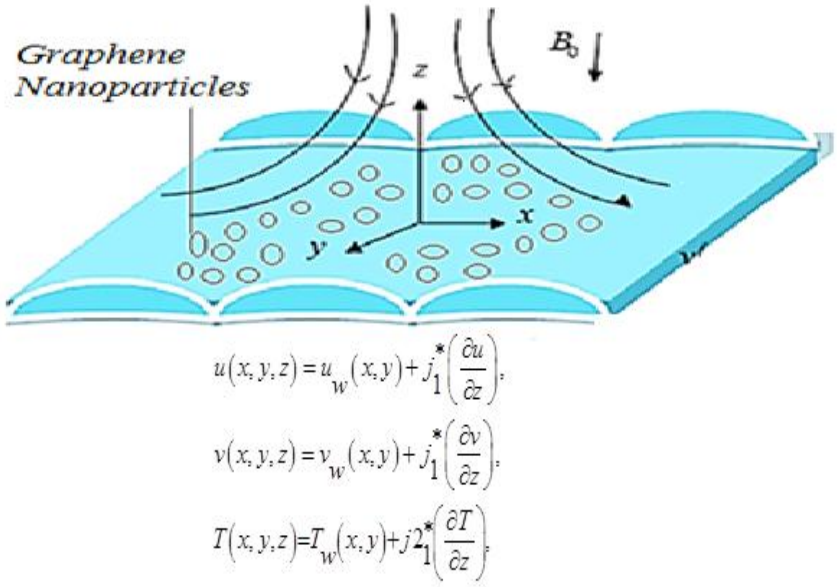

Fig. 1: The physical model of flow over a porous layers slendering sheet

Under the aforesaid assumptions the governing boundary layer equations can be expressed as (Khadar and Megahed [22]; Anjali Devi and Prakash [23]):

$$\frac{\partial u}{\partial x}+\frac{\partial v}{\partial y}+\frac{\partial w}{\partial z}=0, \tag{1}$$

$$\rho_{nf}\left(u\frac{\partial u}{\partial x}+v\frac{\partial v}{\partial y}+w\frac{\partial w}{\partial z}\right)=\mu_{nf}\frac{\partial^2 u}{\partial z^2}-\sigma B_0{}^2u-\frac{\mu_{nf}}{k_0}u, \tag{2}$$

$$\rho_{nf}\left(u\frac{\partial v}{\partial x}+v\frac{\partial v}{\partial y}+w\frac{\partial v}{\partial z}\right)=\mu_{nf}\frac{\partial^2 v}{\partial z^2}-\sigma B_0{}^2v-\frac{\mu_{nf}}{k_0}v, \tag{3}$$

$$\left(\rho C_p\right)_{nf}\left(u\frac{\partial T}{\partial x}+v\frac{\partial T}{\partial y}+w\frac{\partial T}{\partial z}\right)=K_{nf}\frac{\partial^2 T}{\partial z^2}+q''' \tag{4}$$

the appropriate boundary conditions are

$$u\left(x,y\right)=u_w(x,y)+j_1^*\left(\frac{\partial u}{\partial z}\right),v\left(x,y\right)=v_w(x,y)+j_1^*\left(\frac{\partial v}{\partial z}\right)$$
$$T\left(x,y\right)=T_w(x,y)+j_2^*\left(\frac{\partial T}{\partial z}\right), \tag{5}$$

and $u=0,v=0,T=T_\infty,C=C_\infty$ at z=∞,

where $j_1^*=\left[\frac{2-f_1}{f_1}\right]\xi_1\left(x+y+c\right)^{(1-n)0.5},\xi_2=\left(\frac{2\gamma}{\gamma+1}\right)\frac{\xi_1}{\mathrm{Pr}}$ (6)

$$j_2^* = \left[\frac{2-b}{b}\right]\xi_2\left(x+y+c\right)^{(1-n)0.5}, \xi_3 = \left(\frac{2\gamma}{\gamma+1}\right)\frac{\xi_2}{\Pr} \tag{7}$$

$$\left.\begin{aligned} u_w(x,y) &= a(x+y+c)^{(n-1)0.5}, v_w(x,y) = a(x+y+c)^n, \tau = \frac{(\rho C_p)_s}{(\rho C_p)_f} \\ T_w(x,y) &= T_\infty + T_0(x+y+c)^{(1-n)0.5}, \end{aligned}\right\} \text{for } n \neq 1 \tag{8}$$

In the present study, we used the subsequent definitions(Babu and Sandeep [12]):

$$\frac{\mu_{nf}}{\mu_f} = \frac{1}{(1-\phi)^{2.5}}, \frac{\rho_{nf}}{\rho_f} = 1-\phi+\phi r, \frac{(\rho C_p)_{nf}}{(\rho C_p)_f} = (1-\phi)+\phi e, \frac{k_{nf}}{k_f} = 1+\frac{3(k-1)\phi}{k+2},$$

$$\text{where } r = \frac{\rho_s}{\rho_f}, e = \frac{(\rho C_p)_s}{(\rho C_p)_f}, k = \frac{k_s}{k_f}, \sigma = \frac{\sigma_s}{\sigma_f} \tag{9}$$

Now, the following similar transformations are used to transform the non-linear partial differential equations (PDE's) to non-linear ordinary differentia equations (ODE's)

$$\xi = z\left(\frac{(n+1)a}{2\upsilon}\right)^{0.5}\left(x+y+c\right)^{(n-1)0.5} \tag{10}$$

$$T = T_\infty + \left(T_w(x,y) - T_\infty\right)\theta, \tag{11}$$

$$u = a\left(x+y+c\right)^n \frac{\partial f}{\partial \xi}, v = a\left(x+y+c\right)^n \frac{\partial g}{\partial \xi} \tag{12}$$

$$w = -\left(\frac{2av}{n+1}\right)^{0.5}\left(x+y+c\right)^{(n-1)0.5}\left[\frac{n+1}{2}(f+g) + \xi\left(\frac{n-1}{2}\right)\left(\frac{\partial f}{\partial \xi} + \frac{\partial g}{\partial \xi}\right)\right] \tag{13}$$

III. METHOD OF SOLUTION

In view of above similarity transformations the governing partial differential equations are transformed to the following non-linear ordinary differential equations:

$$\frac{1}{(1-\phi)^{2.5}}\frac{n+1}{2}\frac{\partial^3 f}{\partial \xi^3} - \left[(1-\phi)+\phi r\right]\left(n\left(\frac{\partial f}{\partial \xi}\right)^2 + n\frac{\partial f}{\partial \xi}\frac{\partial g}{\partial \xi} - \left(\frac{n+1}{2}\right)(f+g)\frac{\partial^3 f}{\partial \xi^3}\right) - (M + \frac{K}{(1-\phi)^{2.5}})\frac{\partial f}{\partial \xi} = 0 \tag{16}$$

$$\frac{1}{(1-\phi)^{2.5}}\frac{n+1}{2}\frac{\partial^3 g}{\partial \xi^3} - \left[(1-\phi)+\phi r\right]\left(n\left(\frac{\partial g}{\partial \xi}\right)^2 + n\frac{\partial f}{\partial \xi}\frac{\partial g}{\partial \xi} - \left(\frac{n+1}{2}\right)(f+g)\frac{\partial^3 g}{\partial \xi^3}\right) - (M + \frac{K}{(1-\phi)^{2.5}})\frac{\partial g}{\partial \xi} = 0 \tag{17}$$

$$\frac{k_{nf}}{k_s}\frac{\partial^2 \theta}{\partial \xi^2} - \frac{2}{n-1}\Pr\left[(1-\phi)+\phi e\right]\left(\frac{1-n}{2}\left(\frac{\partial f}{\partial \xi} + \frac{\partial g}{\partial \xi}\right)\theta - \left(\frac{n+1}{2}\right)(f+g)\frac{\partial \theta}{\partial \xi}\right) + A^* f' + B^* \theta = 0 \tag{18}$$

and corresponding boundary conditions are

$$\left.\begin{aligned} f(0) &= A\left(\frac{1-n}{n+1}\right)\left[1+ j_1 \frac{\partial^2 f}{\partial \xi^2}\bigg|_{\xi=0}\right],\ f^1(0) = \left[1+ j_1 \frac{\partial^2 f}{\partial \xi^2}\bigg|_{\xi=0}\right], \\ g(0) &= A\left(\frac{1-n}{n+1}\right)\left[1+ j_1 \frac{\partial^2 g}{\partial \xi^2}\bigg|_{\xi=0}\right],\ g^1(0) = \left[1+ j_1 \frac{\partial^2 g}{\partial \xi^2}\bigg|_{\xi=0}\right], \\ \theta(0) &= \left[1+ j_2 \frac{\partial \theta}{\partial \xi}\bigg|_{\xi=0}\right], \\ \frac{\partial f}{\partial \xi} &= 0, \frac{\partial g}{\partial \xi} = 0, \theta = 0, \ \text{as } \xi \to \infty \end{aligned}\right\} \tag{19}$$

$$\text{where } M = \frac{\sigma_f B_0^2}{\rho_f a}, \Pr = \frac{\mu_f (C_p)_f}{k_f}, \ , K = \frac{\mu_f}{\rho_f k_0 a}, j_1 = \frac{2-f_1}{f_1}\xi_1\left(\frac{U_0(m+1)}{2\upsilon}\right)^{1/2},$$

$$j_2 = \frac{2-b}{b}\xi_2\left(\frac{U_0(m+1)}{2\upsilon}\right)^{1/2}, j_3 = \frac{2-d}{d}\xi_3\left(\frac{U_0(m+1)}{2\upsilon}\right)^{1/2} \tag{20}$$

The engineering design quantities of physical interest include the friction factor coefficient, the rate of heat and mass transfer coefficients, and are writes as

$$Cf\left(\mathrm{Re}\right)^{\frac{1}{2}} = 2\left(\frac{n+1}{2}\right)^{0.5}\frac{\partial^2 f}{\partial \zeta^2}\bigg|_{\zeta=0}, \ Nu_x\left(\mathrm{Re}\right)^{-\frac{1}{2}} = -\left(\frac{n+1}{2}\right)^{0.5}\frac{\partial \theta}{\partial \zeta}\bigg|_{\zeta=0}, \tag{21}$$

$$\text{where } \mathrm{Re} = \frac{u_w(x)(x+y+c)}{\upsilon_f}.$$

The non-linear differential Eqs. (16)-(18) with the boundary conditions (19) are solved numerically using Runge-Kutta-Feldberg integration method. Initially, the set of non-linear ODE's converted to first order differential equations, by using the substitution derivatives. Initially, we guess the values ofwhich are not given at the initial conditions. Eqs.(16)-(18) are integrated with help of Runge-Kutta Feldberg integration scheme with the consecutive iterative step length is 0.01. Finally, the present numerical results are validated with the solution of the Khader and Megahed [22] and found worthy agreement with uncertainty of ≤ ±2% (see Table 2).

IV. RESULTS AND DISCUSSION

The dimensionless governing equations (16)-(18) subject to the boundary conditions (19) are solved numerically by using RKF integration scheme. The influence of various flow parameters on momentum, thermal boundary layers as well as the friction factor coefficient, local Nusselt number for graphene-water nanoparticles are studied at two different temperature namely 10^0C and 50^0C through graphs and tables. For numerical computations the non-dimensional parameter values are chosen as $n = 0.65, M = 2,\ j_1 = 0.3,\ j_2 = 0.3,$ $\phi = 0.1, A^* = 0.2, B^* = 0.3,\ Pr = 6.2,$ which are remain unchanged throughout the present simulation. In this section, the solid and dotted lines in the graphs represents the flow in the presence of graphene-water nanoparticle at 10^0C and 50^0C temperature, respectively.

The effect of dimension less velocity slip parameter j_1 on temperature, Azimuthal and Tangential velocity fields are plotted in Figs. 2-4 for the graphene-water nanoparticle at 10^0C and 50^0C temperature. This may happen due to the fact that increase in velocity slip parameter j_1 develops viscous forces, which have

tendency to reduce the momentum boundary layer. It is worth to mentioned that the change of momentum boundary layer in the presence of graphene-water nanoparticle are negligible at 10^0C and 50^0C temperature.

Fig. 5 shows that the effect of dimension less temperature jump parameter j_2 on temperature field decreased for the graphene-water nanoparticle at 10^0C and 50^0C temperature. This may happen due to the fact that increase in temperature jump parameter j_2 develops viscous forces, which have tendency to reduce the thermal boundary layer in the presence of graphene-water nanoparticle are negligible at 10^0C and 50^0C temperature.

Figs. 6 and 7 display the impact of space and temperature dependent heat source or sink parameter A^* and B^* on dimensional temperature field. It is evident that from the Figs. 6 and 7, the rising values of A^* and B^* enhanced the temperature fields for both 10^0C and 50^0C temperature of graphene-water nanoparticle cases. It is well known that the positive values of A^* and B^* indicate the heat generation while negative values represent the heat absorption of the system. It is worth to mention that at lower temperature (10^0C) of graphene-water nanoparticle is slightly increased very close to boundary layer ($\zeta \leq 0.65$) with the increment in B^*.

Figs. 8-10 are plotted to examine the influence of magnetic field parameter M on the velocity and temperature profiles. It can be found that increasing values of M decelerates the velocity profile (Figs. 8 and 9). From these we observed that the effects of transverse magnetic field on electrically, conducting fluid give rise to resistive-type force called Lorentz force. This force has tendency to slow down the motion of the fluid in the boundary layer. These results quantitatively agree with the expectations, since magnetic field M exerts retarding force on natural convection flow, while the magnetic field parameter M increases in temperature field as shown in Fig.10 in the presence of graphene-water nanoparticle at 10^0C and 50^0C temperature.

Figs. 11 and 12 illustrate the effect of porosity parameter *K* on velocity profiles along the tangential and azimuthal direction of the flow for the graphene-water nanoparticles at 10^0C and 50^0C temperature, respectively. It is found that enhancing the porosity parameter attenuate the thickness of both tangential and azimuthal velocity fields. This is because the holes of the porous layers expand with an increase in the porosity parameter and reduce the thickness of the momentum boundary layer. While the reverse behaviour can be found in temperature field shown in Fig.13.

From Fig. 14, it is evident that for higher values of nanofluid volume fraction ϕ enhance the temperature profile due to increasing the thermal conductivity caused by the suspended graphene-water nanoparticles at 10^0C and 50^0C temperature. Figs. 15-17 display the influence of wall thick mess parameter A on velocity and temperature profiles of the flow for graphene-water nanoparticle at different temperature. With the increase in the wall thickness parameter we observed momentum and thermal boundary layer thickness decreases.

Table 3 displays the deviation in skin friction coefficient and local Nusselt number with various values of velocity slip parameter, temperature jump parameter, the space and temperature dependent heat source/sink parameter, magnetic field parameter, porosity parameter, volume fraction and wall thickness parameter for graphene-water nanoparticle at 10^0C and 50^0C temperature. It is found that $j_2, A^*, B^*, M, K, \phi$ decreases the local skin friction coefficient and heat transfer rate. It is observed that both friction factor coefficients decrease with an increase of nanoparticle volume fraction while same phenomena can observe in Nusselt number. On contrast, the velocity parameter j_1 enhances friction factor coefficients and reverse trend can be observed in heat transfer rate. In addition, we can observe that the friction factor coefficients decelerates with increase in values of wall thickness parameter A while opposite phenomena can be obtained in Nusselt number in the case of graphene-water nanoparticles cases at different temperature namely 10^0C and 50^0C.

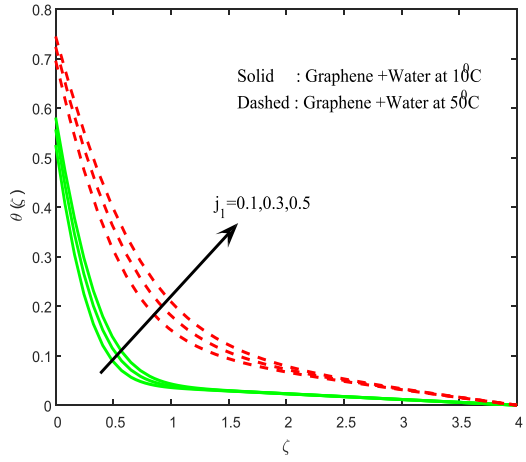

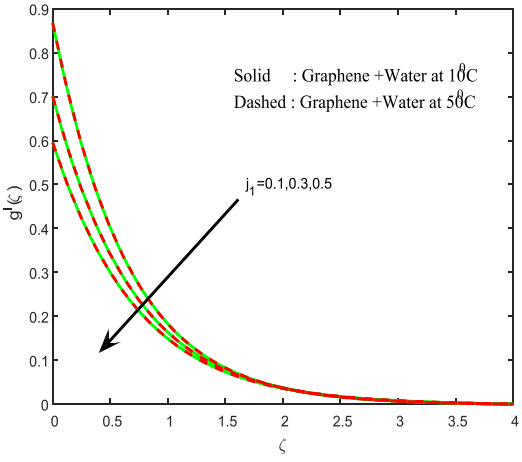

Fig.2Temperature field for different values of j_1

Fig.3 Azimuthal velocity field for different values of j_1

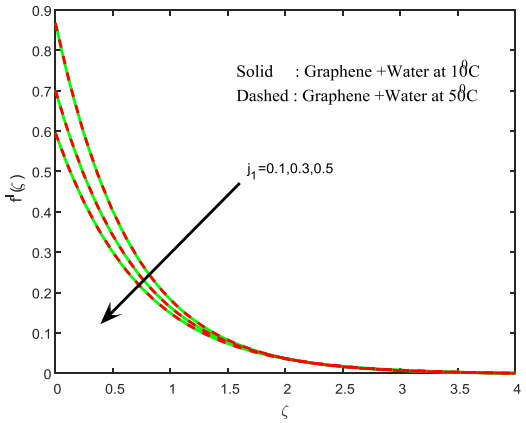

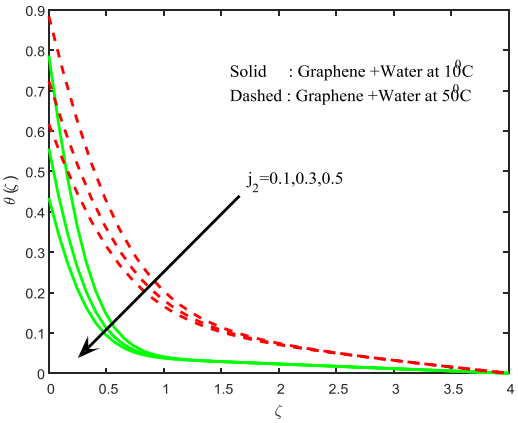

Fig.4 Tangential velocity field for different values of j_1

Fig.5 Temperature field for different values of j_2

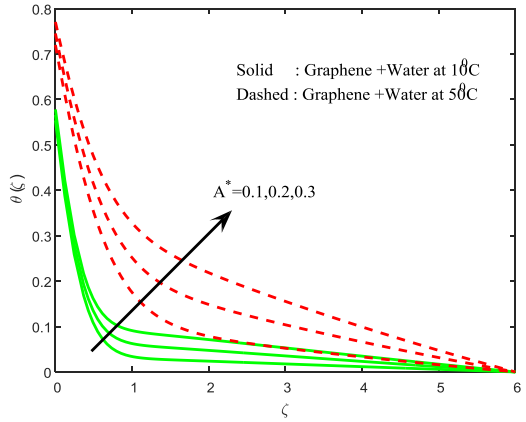

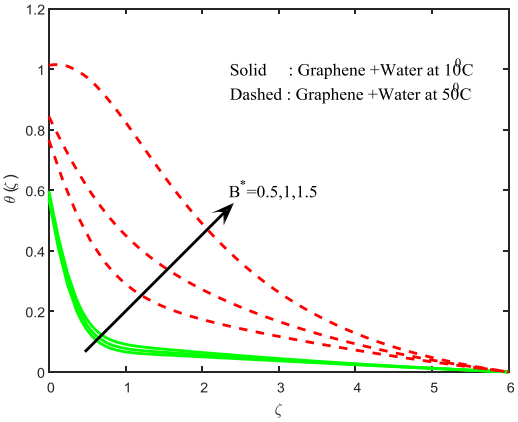

Fig.6 Temperature field for different values of A^*

Fig.7 Temperature field for different values of B^*

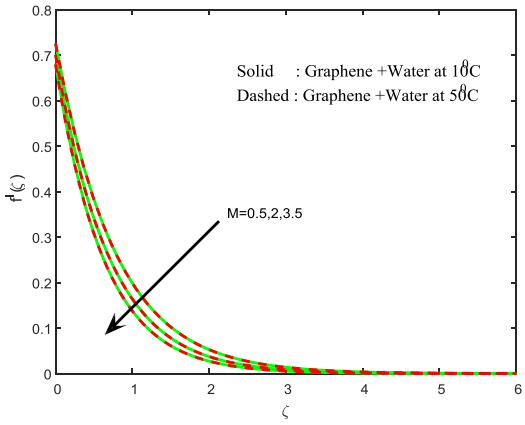

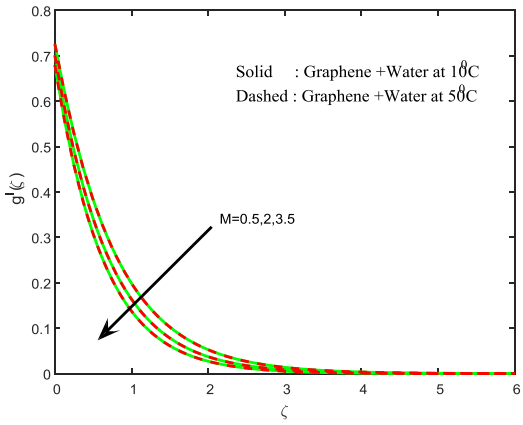

Fig.8 Tangential velocity field for different values of M

Fig.9 Azimuthal velocity field for different values of M

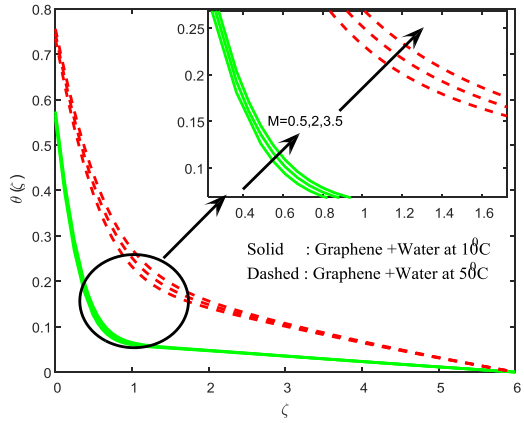

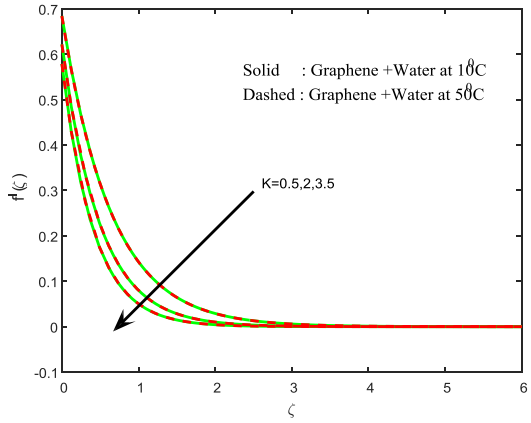

Fig.10 Temperature field for different values of M

Fig.11 Tangential velocity field for different values of K

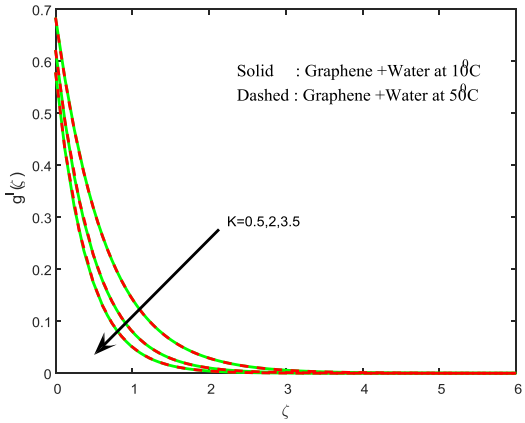

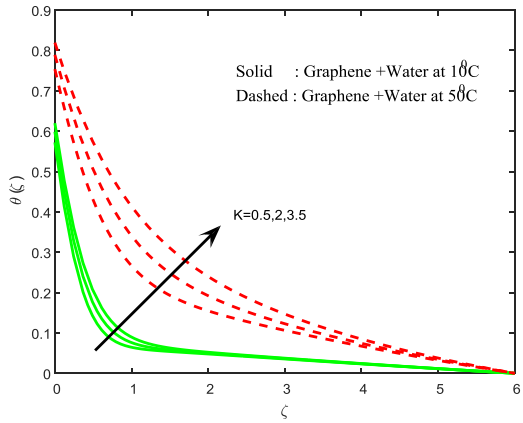

Fig.12 Azimuthal velocity field for different values of K

Fig.13 Temperature field for different values of K

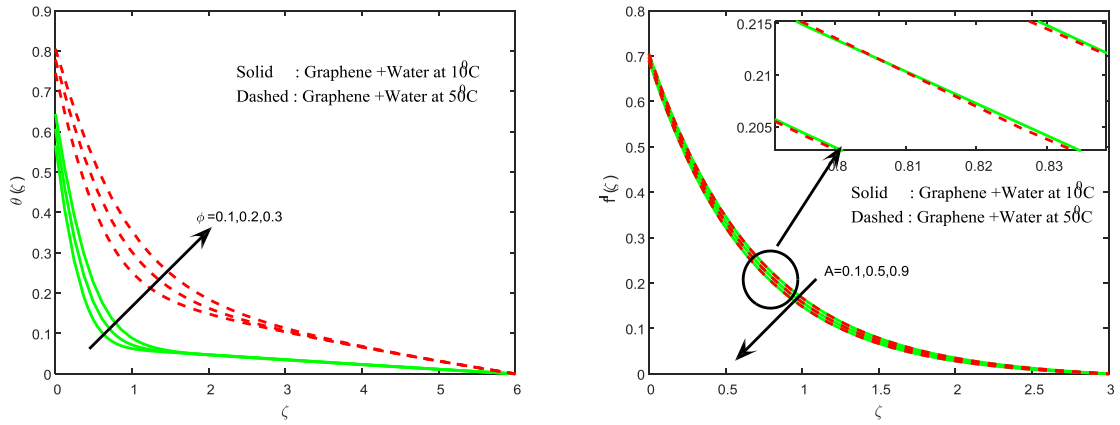

Fig.14 Temperature field for different values of ϕ

Fig.15 Tangential velocity field for different values of A

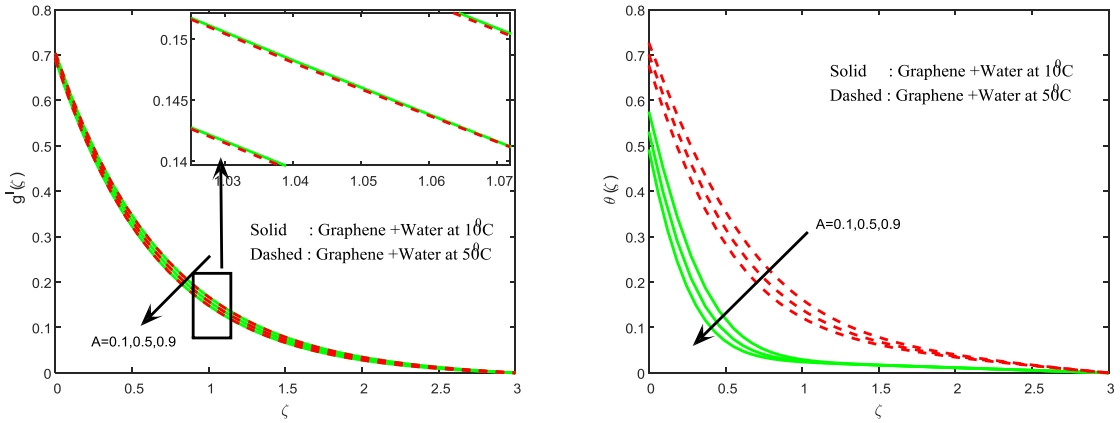

Fig.16 Azimuthal velocity field for different values of A

Fig.17 Temperature field for different values of A

V. CONCLUSIONS

The present computational results characterize the effects ofMagnetic field parameter on three dimensional (3D)nanofluid flows across slendering sheet in porous layers with non-uniform heat source/sink by considering the graphene-water nanoparticles at 10^0C and 50^0C temperature. The resultant non-linear governing partial differential equations (PDEs) are solved using the robust RKF integration method. Based on the present computational investigation the following observations are made:

- The wall thickness parameter decelerates in friction factor coefficients while enhances in heat transfer rate.
- A rise in porosity parameter enhances then reduces the rate of heat transfer.
- Increase in the values of nanoparticle volume fraction parameter decreases in both friction factor coefficients while same phenomena see in heat transfer rate.
- The temperature of the fluid is high in case of graphene-water nanoparticles at 50^0C compared to the graphene-water nanoparticle at 10^0C temperature.

NOMENCLATURE

u, v, w : Velocity components in x, y and z directions
C_p : Specific heat capacity at constant pressure
f, g : Dimensionless velocities
A : Coefficient related to stretching sheet
m : Velocity power index parameter
$B(x)$: Magnetic field parameter
T : Temperature of the fluid
k : Thermal conductivity
T_m : Mean fluid temperature
T_∞ : Temperature of the fluid in the free stream
C_∞ : Concentration of the fluid in the free stream
j_1^* : Dimensional velocity slip parameter
j_2^* : Dimensional temperature jump parameter
ϕ : Volume fraction parameter
f_1 : Maxwell's reflection coefficient
A^*, B^* :Space and temperature dependent heat source/sink parameter
a : Thermal accommodation coefficient
b : Physical parameter related to stretching sheet
m : Velocity power index parameter
$\Pr$: Prandtl number
q''' : Non-uniform heat source/sink parameter
$B(x)$: Dimensional magnetic field parameter
M : Magnetic interaction parameter
K : Porosity parameter
Le : Lewis number
Nb : Brownian motion parameter
j_1 : Dimensionless velocity slip parameter
j_2 : Dimensionless temperature jump parameter
C_f : Wall skin friction coefficient
Nu_x : Local Nusselt number
Re_x : Local Reynolds number

Greek Symbols

η : Similarity variable
σ : Electrical conductivity of the fluid
γ : Ratio of specific heats
θ : Dimensionless temperature
ρ_{nf} : Density of the nanofluid

k_{nf} : Thermal conductivity of the nanofluid

μ_{nf} : Dynamic viscosity of nanofluid

υ_f : Kinematic viscosity

A : Wall thickness parameter

ξ_1, ξ_2 : Mean free path (constant)

ξ_3 : Mean free path (constant)

Table 1: Thermo physical properties of base fluid and nano particles at different temperatures

Name	ρ (Kg/m^3)	c_p (JK/gK)	k (W/mK)	Pr	Temp $in\ ^0C$
H_2O	999.6	4090	0.5884	8.80	10
H_2O	987.7	4066	0.6440	3.35	50
Graphene	2250	2100	2500	-	-

Table 2: Validation of the present values of $F''(0)$ when $K = M = A^* = B^* = Nb = Nt = \phi = Le = 0, \beta \to \infty, n = 0.5$

δ	j_1	Khader and Megahed [22]	Present study
0.2	0	-0.924828	-0.924829
0.25	0.2	-0.733395	-0.733396
0.5	0.2	-0.759570	-0.759570

Conflict of interest

The authors declare that there is no conflict of interests regarding the publication of this paper.

References

[1] S. W. Lee, S. S. Lee, and E. H. Yang, Nanoscale, Research Letters, 4, 1218, 2009.

[2] A. Malesevic, R. Kemps, A. Vanhulsel, P. M. Chowdhury, V. Alexander, and V. H.Chris, "Field emission from vertically aligned few-layer graphene", Journal of Applied Physics, 104, 084301, 2008.

[3] S.Ghosh, D L.Nika, E P.Pokatilovand, and A A. Balandin, "Heat conduction in graphene: experimental study and theoretical interpretation",New Journal of Physics, 1,1095012,2009.

[4] L. F. Mao, Carbon, 49, 2709, 2011.

[5] TessyTheres Baby and Sundara Ram prabhu, "Experimental study on the field emission properties of metal oxide nanoparticle-decorated graphene", Journal of Applied Physics,111, 034311, 2012, doi: 10.1063/1.3681376.

[6] A. K. M, MahmudulHaque, Sunghyun Kwon, Junhyo Kim, Jungpil Noh, Sunchul Huh, Hanshik Chung, and HyominJeong, "An experimental study on thermal characteristics of nanofluid with graphene and multi-wall carbon nanotubes", Journal of Central South University of Technology,22: 3202−3210, 2015,DOI: 10.1007/s11771-015-2857-3.

[7] R. Cortell, "MHD (magneto-hydrodynamic) flow and radiative nonlinear heat transfer of a viscoelastic fluid over a stretching sheet with heat generation/absorption", Energy, 74,896-905, 2014,doi.org/10.1016/j.energy.2014.07.069.

[8] C.S.K. Raju, N. Sandeep, V. Sugunamma, M. JayachandraBabu, and J.V. Ramana Reddy, "Heat and mass transfer in magnetohydrodynamic Casson fluid over an exponentially permeable stretching surface", Engineering Science and Technology,an International Journal, 19,45-52, 2016, dx.doi.org/10.1016/j.jestch.2015.05.010. 69-75.

[9] T. Hayat, M. Imtiaz, A. Alsaedi, and M.A. Kutbi, "MHD three dimensional flow of nanofluid with velocity slip and nonlinear thermal radiation", Journal of Magnetism and Magnetic Materials, 396,31-37, 2015,doi.org/10.1016/j.jmmm.2015.07.091.

[10] I.L. Animasaun, C.S.K. Raju, and N. Sandeep, "Unequal diffusivities case of homogeneous–heterogeneous reactions within viscoelastic fluid flow in the presence of induced magnetic-field and nonlinear thermal radiation", Alexandria Engineering Journal, 55, 1595-1606, 2016.

[11] E. Nelson, "Dynamical theories of Brownian motion", Mathematical Notes, 131,2381-2396, 1967,http://dx.doi.org/10.1103/PhysRev. 131.2381.

[12] M. Jayachandra Babu, and N. Sandeep , "3D MHD slip flow of a nanofluid over a slendering stretching sheet with thermophoresis and Brownian motion effects", Journal of Molecular Liquids, 222, 1003-1009,2016.
[13] S.U.S. Choi, "Enhancing thermal conductivity of fluids with nanoparticles", International Mechanical Engineering Congress and Exposition, San Francisco, 66, ASME, 99-105,1995.
[14] M. Sheikholeslami, and D.D. Ganji, "Nanofluid flow and heat transfer between parallel plates considering Brownian motion using DTM", Computer Methods Applied Mechanics and Engineering 283,651-663,2015, doi.org/10.1016/j.cma.2014.09.038.
[15] A. Malvandi, S. Heysiattalab, and D.D. Ganji, "Thermophoresis and Brownian motion effects on heat transfer enhancement at film boiling of nanofluids over a vertical cylinder", Journal of Molecular Liquids, 216, 503-509, 2016, doi.org/10.1016/j.molliq.2016.01.030.
[16] B. Fani, M. Kalteh, and A. Abbassi, "Investigating the effect of Brownian motion and viscous dissipation on the nanofluid heat transfer in a trapezoidal micro channel heat sink", Advanced Powder Technology, 26,83-90, 2015, doi.org/10.1016/j.apt.2014.08.009.
[17] S.A. Angayarkanni, and John Philip, "Review on thermal properties of nanofluids: Recent developments", Advances in colloid and Interface science, 225, 146-176, 2015.
[18] WA Khan, A Aziz,"Natural convection flow of a nanofluid over a vertical plate with uniform surface heat flux", International Journal of Thermal Sciences, 50, 1207-14, 2011.
[19] S. Das, R.N. Jana, and O.D. Makinde**, "**Mixed convective magnetohydrodynamic flow in a vertical channelfilled with nanofluids", Engineering Science and Technology, an International Journal, 18, 2015, 244e255.
[20] OD. Makinde and Adetayo S. Eegunjobi, "Entropy analysis of thermally radiating magnetohydrodynamic slip flow of Cassonfluid in a microchannel filled with saturated porous media" ,Journal of Porous Media, 19, 799-810, 2016.
[21] J. Kim, Y.T. Kang, and C.K. Choi, "Analysis of convective instability and heat transfer characteristics of nanofluids", Physics of Fluids, 16, 2395-2401, 2004.
[22] M. Khader, and A.M. Megahed, "Numerical solution for boundary layer flow due to a nonlinearly stretching sheet with variable thickness and slip velocity", European Physical Journal Plus, 128, 100-108,2003.
[23] S.P. Anjali Devi, and M. Prakash, "Slip flow effects over hydromagnetic forced convective flow over a slendering stretching sheet", Journal of Applied Fluid Mechics, 9, 683-692,2016.
[24] C. S. K.Rajuand N. Sandeep, "Unsteady Casson nanofluid flow over a rotating cone in a rotating frame filled with ferrous nanoparticles: A numerical study", Journal of Magnetism and Magnetic Materials, 421, 216-224,2017.
[25] S. Das, R. N.Jana, R.P. Sharma, O.D. Makinde, "MHD Nanofluid Flow and Heat Transfer in Ekman Layer on an Oscillating Porous Plate", Journal of Nanofluids, 5, 968-981,2016.
[26] C. S. K. Raju, K. R. Sekhar, S. M. Ibrahim, G. Lorentzini, G. Viswanatha Reddy, and E. Lorentzini, "Variable viscosity on unsteady dissipative Carreau fluid over a truncated cone filled with titanium alloy nanoparticles", Continuum Mechanics and Thermodynamics, DOI 10.1007/s00161-016-0552-8.
[27] A. G. Madaki, R. Roslan, M. S. Rusiman, and C.S. K. Raju, "Analytical and numerical solutions of squeezing unsteady Cu and TiO2-nanofluid flow in the presence of thermal radiation and heat generation/absorption", Alexandria Engineering Journal, doi.org/10.1016/j.aej.2017.02.011.

Table 3: Variation of Friction factor coefficients, Nusselt number for different non-dimensional parameters with graphene-water nanoparticles at 10^0C and 50^0C temperature.

j_1	j_2	A^*	B^*	M	K	ϕ	A	Friction factor coefficient		Friction factor coefficient		Nusselt number	
								Graphene-water at 10^0C	Graphene-water at 50^0C	Graphene-water at 10^0C	Graphene-water at 50^0C	Graphene-water at 10^0C	Graphene-water at 50^0C
0.1								-1.318554	-1.319410	0.868145	0.868059	1.581736	1.014313
0.3								-0.996579	-0.997035	0.701026	0.700890	1.476681	0.921350
0.5								-0.808605	-0.808890	0.595698	0.595555	1.397049	0.851486
	0.1							-0.996579	-0.997035	0.701026	0.700890	2.126279	1.156674
	0.3							-0.996579	-0.997035	0.701026	0.700890	1.476681	0.921350
	0.5							-0.996579	-0.997035	0.701026	0.700890	1.131114	0.765591
		0.1						-0.996469	-0.996926	0.701059	0.700922	1.487099	0.932904
		0.2						-0.996469	-0.996926	0.701059	0.700922	1.446601	0.848511
		0.3						-0.996469	-0.996926	0.701059	0.700922	1.406104	0.764119
			0.5					-0.996469	-0.996926	0.701059	0.700922	1.431475	0.780146
			1.0					-0.996469	-0.996926	0.701059	0.700922	1.389583	0.520850
			1.5					-0.996469	-0.996926	0.701059	0.700922	1.340486	-0.043791
				0.5				-0.913781	-0.914341	0.725866	0.725698	1.475793	0.886153
				2.0				-0.996469	-0.996926	0.701059	0.700922	1.446601	0.848511
				3.5				-1.066729	-1.067113	0.679981	0.679866	1.420201	0.813913
					0.5			-1.052206	-1.052604	0.684338	0.684219	1.425786	0.821278

					2.0			-1.260586	-1.260824	0.621824	0.621753	1.338237	0.703026
					3.5			-1.403647	-1.403812	0.578906	0.578856	1.267098	0.602158
						0.1		-0.996469	-0.996926	0.701059	0.700922	1.446601	0.848511
						0.2		-1.031251	-1.031880	0.690625	0.690436	1.309085	0.739083
						0.3		-1.036694	-1.037366	0.688992	0.688790	1.186629	0.649393
							0.1	-0.985290	-0.985723	0.704413	0.704283	1.415105	0.910327
							0.5	-1.009434	-1.009909	0.697170	0.697027	1.562212	0.995063
							0.9	-1.033420	-1.033937	0.689974	0.689819	1.693161	1.075743